

# Investigating Sparse Reconfigurable Intelligent Surfaces (SRIS) via Maximum Power Transfer Efficiency Method Based on Convex Relaxation

Hans-Dieter Lang\*, Michel A. Nyffenegger\*, Heinz Mathis\*, and Xingqi Zhang†

\*OST – Eastern Switzerland University of Applied Sciences, Rapperswil, SG, Switzerland. Email: hansdieter.lang@ost.ch

†School of Electrical and Electronic Engineering, University College Dublin, Dublin, Ireland.

**Abstract**—Reconfigurable intelligent surfaces (RISs) are widely considered to become an integral part of future wireless communication systems. Various methodologies exist to design such surfaces; however, most consider or require a very large number of tunable components. This not only raises system complexity, but also significantly increases power consumption. Sparse RISs (SRISs) consider using a smaller or even minimal number of tunable components to improve overall efficiency while maintaining sufficient RIS capability. The versatile semidefinite relaxation-based optimization method previously applied to transmit array antennas is adapted and applied accordingly, to evaluate the potential of different SRIS configurations. Because the relaxation is tight in all cases, the maximum possible performance is found reliably. Hence, with this approach, the trade-off between performance and sparseness of SRIS can be analyzed. Preliminary results show that even a much smaller number of reconfigurable elements, e.g. only 50%, can still have a significant impact.

**Index Terms**—Reconfigurable Intelligent Surface (RIS), Meta-surface, Scattering, Optimization Methods, Loaded Antennas.

## I. INTRODUCTION

Reconfigurable intelligent surfaces (RISs) continue to gain interest in many research areas including applied electromagnetics, antennas & propagation, and mobile communications [1]–[4]. They are widely considered to play a key role in future wireless communication technologies and networks, such as “beyond 5G”, 6G, and onwards [5]–[7].

The main idea builds on reconfigurable reflectarrays [8]: RIS divert otherwise unused (“spilled”) wireless signals back into the system, to enhance coverage and throughput of wireless links. In order for the reflection to be useful, these reflectors must be both reconfigurable and “intelligent”, i.e., they must be controlled to optimize the overall performance for each link, taking into account all the users involved as well as the entire channel, including all other scatterers. Such smart reflectors should reduce the need for additional base stations and save both costs and energy. Therefore, the use of RIS should not only improve system performance per cost, but also overall energy efficiency and sustainability.

The last point is one of many challenges associated with this technology. The premise is that such RISs constitute (much) more power-efficient network components than additional fully functional base stations. RIS are considered to be low-power and low-cost [9]. However, they are not entirely passive, as

they must contain tunable elements. Various tuning mechanisms have been considered [10]. For applications below optical and mmWave frequency ranges, most importantly biased varactor diodes are used as tunable capacitors. And while each varactor diode can be considered low-power, a large number of them can still add up to a considerable amount of power required for the operation of the RIS (in addition to the power consumption of the central control engine).

## II. SPARSE RIS (SRIS)

A large number of tunable elements clearly increases the number of degrees of freedom for accuracy and focusing of the reflected beam (possibly to many users at the same time, at different frequencies or in different time slots). However, this not only increases the system complexity when it comes to setting all these elements correctly (i.e., with an optimization algorithm), but also the total power consumption of the RIS. Therefore, one of the criticisms is that such RIS are not necessarily simpler and at least not much more energy efficient than additional base stations.

Hence, the goal is to reduce the number of tunable elements required, to improve the energy efficiency of the RIS. The result is an RIS with sparsely populated tunable elements, a so-called Sparse RIS (SRIS). Sparse RISs (SRISs) consider using a smaller or even minimal number of such tunable components to improve efficiency while maintaining sufficient RIS capability. At this stage, it is unclear which strategy will best accomplish this. The most commonly used techniques to design RISs, see, e.g., [5], [11], seem not directly applicable.

This is where the optimization procedure adopted from array antennas, as described in the following, comes in: Both to assess the performance of a particular RIS design as well as to investigate the effects of reducing the number of tunable elements on an RIS, e.g., by clustering or simply removing some tunable elements, a method is desired that give the maximum enhancement for a given use case.

Note that, beyond the intrinsic sparsity of RISs, employing sparsity also in the deployment of these SRISs further improves sustainability, by minimizing both manufacturing costs and resource consumption, as well as overall energy consumption. However, this is not a topic for this work.

### III. OPTIMIZATION PROCEDURE

The following optimization procedure is based on a framework originally developed for wireless power transfer (WPT) in the near-field [12], [13], which has subsequently been adapted for far-field applications [14]. More recently also sidelobe and backlobe constraints have been added [15], which are beyond the scope of this paper, but are generally interesting for (S-)RIS analysis as well.

The overall objective of the method is to find the optimal feasible currents in all antenna elements that minimize the total transmit power required to obtain unity power in the receive antenna. For this purpose, the entire SRIS setup is simulated as a multiport network to obtain its impedance matrix. The required Kirchhoffs Voltage Law (KVL) and power equations are then all formulated using standard circuit network analysis based on that matrix. For the SRIS to be passive, all average transferred powers at RIS element ports are required to be zero, while the transmit power is minimized.

Note that this method is by no means limited to surfaces considering reflection only; it may just as well be applied to analyze transmitting surfaces or surfaces that simultaneously transmit and reflect, e.g., STAR-RIS [16], [17]. Furthermore, the method can also be used to assess the performance of a particular RIS design, when using reactively loaded RIS elements (instead of geometrically adjusting the elements to achieve essentially the same reactive behavior).

#### A. Prerequisites

The overview of the problem is visualized in Fig. 1 and an example of such a setup, which is going to serve as test case, is shown in Fig. 2. In essence, it all boils down to a multiport network problem of transferring maximum power from the transmit port (tx) to the receiver port (rx) with the help of the rest of the network when all other ports are only connected by lossless reactances.

Let the impedance matrix  $\mathbf{Z}$  of the entire (unoptimized) wireless link consisting of the transmit antenna, RIS, and receive antenna be partitioned according to

$$\mathbf{Z} = \begin{bmatrix} z_t & \mathbf{z}_{ts} & z_{tr} \\ \mathbf{z}_{ts}^T & \mathbf{Z}_s & \mathbf{z}_{sr} \\ z_{tr} & \mathbf{z}_{sr}^T & z_r \end{bmatrix} \in \mathbb{C}^{(N+2) \times (N+2)}, \quad (1)$$

where  $N$  stands for the number of antennas (ports) of the RIS which contain tunable elements. The subscripts  $t$ ,  $s$ , and  $r$  refer to the transmitter antenna port, the  $N$  surface antennas and the receiver antenna, respectively. The subscript combinations  $ts$ ,  $tr$ , and  $sr$  stand for the coupling of the respective elements. Due to reciprocity, the matrix is symmetric with respect to its main diagonal, and  $\mathbf{Z} = \mathbf{Z}^T$  as well as  $\mathbf{Z}_s = \mathbf{Z}_s^T$ .

The vectors of currents and voltages associated with this impedance matrix system are partitioned accordingly, i.e.,  $\mathbf{i}^T = [i_t, \mathbf{i}_s^T, i_r]$  and  $\mathbf{v}^T = [v_t, \mathbf{v}_s^T, v_r]$  where  $\mathbf{i}, \mathbf{v} \in \mathbb{C}^{N+2}$ .

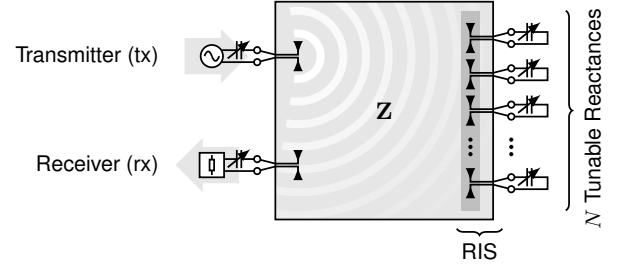


Fig. 1. The multiport network to model the wireless link between transmitter, receiver and the RIS, where the goal is to maximize power transfer from the transmitter to the receiver using optimally tuned reactances.

#### B. Objective: Power Transfer Efficiency, Power Gain, Antenna Gain, and Bistatic Radar Cross Section

Using the aforementioned quantities, the *Power Transfer Efficiency* (PTE)  $\eta$  of the reduced two-port network can be formulated from the ratio of received and transmitted power according to

$$\eta = \frac{P_r}{P_t} = \frac{\frac{1}{2}|i_r|^2 R_{rx}}{\frac{1}{2} \operatorname{Re}(\mathbf{i}^H \mathbf{v})} = \frac{|i_r|^2 \operatorname{Re} z_r}{\mathbf{i}^H (\operatorname{Re} \mathbf{Z}) \mathbf{i}}, \quad (2)$$

where due to conjugate-matched transmit and receive antennas, the receiving resistance is  $R_{rx} = \operatorname{Re} z_r$ . Under these conditions, the *Power Gain*  $g$  of the reduced two-port network can be expressed in terms of S-parameters of the two-port network and antenna parameters as follows:

$$g = \frac{P_r}{P_t} = \frac{|S_{21}|^2}{1 - |S_{11}|^2} = \frac{G'_{tx} G_{rx}}{L_{FS}} = \frac{G_{tx} G_{rx}}{L_{FS}} \frac{\sigma_B}{4\pi d^2}. \quad (3)$$

$G_{tx}$  and  $G_{rx}$  refer to the gains of the transmitter and receiver antenna, respectively,  $\sigma_B$  is the bistatic radar cross section (BRCS) of the reflector, such that the combined transmitter gain is  $G'_{tx} = G_{tx} \sigma_B / (4\pi d^2)$ , and  $L_{FS} = (4\pi d / \lambda)^2$  is the free-space loss over the distance  $d$  at the free-space wavelength  $\lambda$ . Hence, optimizing the PTE  $\eta$  is equivalent to optimizing the power gain  $g$ , which in turn is equivalent to optimizing the total transmit antenna gain  $G'_{tx}$  or the BRCS  $\sigma_B$  of the RIS.

#### C. Constraints

1) *KVL at the Receiver*: On the receiver end, impedance-matched conditions lead to the KVL

$$[z_{tr}, \mathbf{z}_{sr}^T, 2 \operatorname{Re} z_r] \mathbf{i} = 0. \quad (4)$$

And to obtain a well-defined problem, all phases are expressed in reference to the receiver current by setting  $\operatorname{Im} i_r = 0$  (via constraint or by reducing the vector of variables accordingly).

The entire optimization problem is first formulated in terms of a (real-valued) vector of unknowns, corresponding to the real and imaginary parts of the currents  $\mathbf{c}^T = [\operatorname{Re} \mathbf{i}^T, \operatorname{Im} \mathbf{i}^T]$  (and similarly for the voltage). KVL and the phase condition can be ensured within affine equality constraints  $\mathbf{A} \mathbf{c} = \mathbf{b}$ .

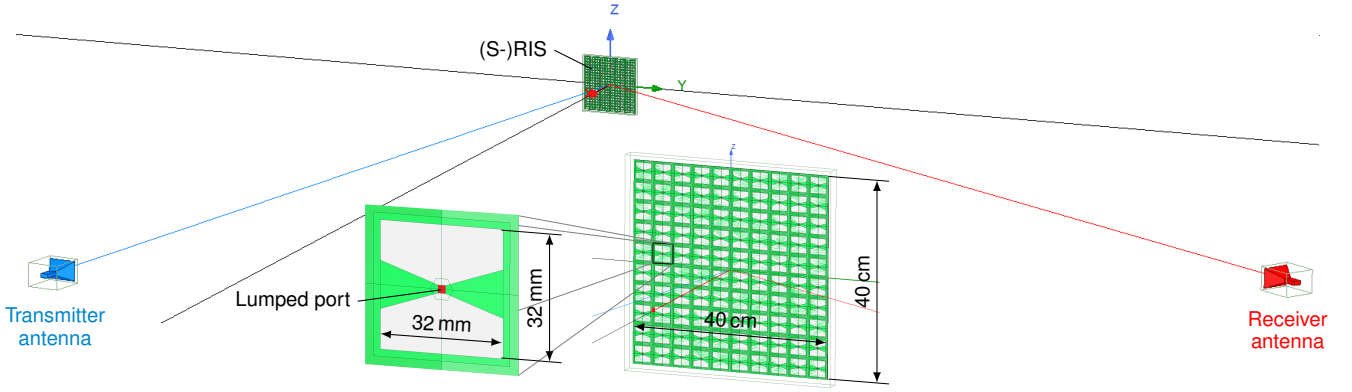


Fig. 2. Simulation setup of the test cases in ANSYS HFSS: The transmitter antenna (blue, left) is at an angle  $10^\circ$  off broadside, the receiving antenna (red, right) is at various angles  $\alpha$  off broadside and  $1^\circ$  below the  $xy$ -plane. The RIS consists of  $10 \times 10 = 100$  vertically polarized printed dipoles.

2) *Passivity of RIS-Elements*: The goal of the optimization procedure is to find the optimally tuned reactances by maximizing the received power while maintaining zero real-power constraints at all ports other than the transmitter and the receiver, i.e., at all RIS antenna ports:

$$P_n = \frac{1}{2} \mathbf{c}^T \mathbf{Q}_n \mathbf{c} = 0, \quad \forall n \in [2, N + 1]. \quad (5)$$

Each  $\mathbf{Q}_n$  corresponds to the  $n^{\text{th}}$  real-valued port impedance matrix. They can be directly formulated from the impedance matrix  $\mathbf{Z}$  [12], noting two typos corrected in [13]. However, since each  $\mathbf{Q}_n$  is an indefinite matrix, (5) amounts to  $N$  nonconvex quadratic equality constraints.

Requiring zero real power to be transferred via these ports, means that only reactive power can be exchanged. The corresponding optimal reactive termination for each port  $n$  (i.e., each RIS element) is found by

$$x_n^* = -\text{Im}(v_n^*/i_n^*), \quad (6)$$

where  $v_n^*$  is the optimal unloaded voltage, found from the optimal currents and the impedance matrix via  $\mathbf{v}^* = \mathbf{Z}\mathbf{i}^*$ . Note that the superscript stars denote optimal quantities, not complex conjugates.

3) *Optional Additional Constraints*: Additional constraints could be added to ensure impedance matching. While that is crucial for optimizing transmit array antennas, it is not required here. Both transmit and receive antennas will be designed to be matched anyway. Furthermore, side- and/or back-lobe constraints may be added by including additional receiving antennas in the model in the desired directions/locations. This could be interesting for (S-)RIS applications, but is beyond the scope of this paper.

#### D. Optimization Problem Formulation

The following simple Quadratically Constrained Quadratic Program (QCQP) is obtained by combining all these constraints and the cost function:

$$\begin{aligned} P_{t,\min}^{\text{QCQP}} = \min_{\mathbf{c}} P_{\text{in}} &= \frac{1}{2} \mathbf{c}^T (\sum_n \mathbf{Q}_n) \mathbf{c} \\ \text{s.t. } P_n &= \frac{1}{2} \mathbf{c}^T \mathbf{Q}_n \mathbf{c} = 0, \quad n \in [2, N + 1] \\ \mathbf{A}\mathbf{c} &= \mathbf{b}. \end{aligned} \quad (7)$$

However, this QCQP is *nonconvex*. It belongs to the class of problems known to be notoriously difficult to solve. Such problems are frequently referred to as “unsolvable”, because the computational cost can quickly exceed any feasible means, at least for a large number of variables.

#### E. Semidefinite Relaxation (SDR)

From the nonconvex QCQP (7), a Semidefinite Program (SDP) [18] can be formulated in terms of the current matrix  $\mathbf{C} = \mathbf{c}\mathbf{c}^T$  using the cyclic permutation property of the trace  $\mathbf{c}^T \mathbf{Q} \mathbf{c} = \text{tr}(\mathbf{c}^T \mathbf{Q} \mathbf{c}) = \text{tr}(\mathbf{Q} \mathbf{c} \mathbf{c}^T) = \text{tr}(\mathbf{Q} \mathbf{C})$ , resulting in:

$$\begin{aligned} P_{t,\min}^{\text{SDR}} &= \min_{\mathbf{C}, \mathbf{c}} \frac{1}{2} \text{tr}(\sum_n \mathbf{Q}_n \mathbf{C}) \\ \text{s.t. } \text{tr}(\mathbf{Q}_n \mathbf{C}) &= 0, \quad n \in [2, N + 1] \\ \mathbf{A}\mathbf{c} &= \mathbf{b} \\ \begin{bmatrix} \mathbf{C} & \mathbf{c} \\ \mathbf{c}^T & 1 \end{bmatrix} &\succeq 0. \end{aligned} \quad (8)$$

The programs (7) and (8) are in general not completely equivalent. That would require that  $\mathbf{C} - \mathbf{c}\mathbf{c}^T = 0$ . However, this condition is equivalent to both  $\mathbf{C} - \mathbf{c}\mathbf{c}^T \succeq 0$  and  $\mathbf{C} - \mathbf{c}\mathbf{c}^T \preceq 0$ . The elimination of the second of these two constraints is the typical semidefinite relaxation applied to obtain a solvable convex SDP. Such programs are reliably and efficiently solvable, even for a (reasonably) large number of variables, using dedicated algorithms, such as SDPT3 [19].

#### F. Tightness of the Problem

A test has to confirm whether the optimum solution of the SDP (8) actually coincides with the optimum of the original QCQP (7). To check for this desired property, the following (relative) *tightness error* (TE) [12], is used:

$$\epsilon = \|\mathbf{C}^* - \mathbf{c}\mathbf{c}^T\| / (\mathbf{c}^T \mathbf{c}). \quad (9)$$

If  $\epsilon$  is sufficiently small, the relaxation was *tight* and the solution of the SDP (8) corresponds to the solution of the original nonconvex QCQP (7).

However, if that is not the case, the obtained solution is infeasible with respect to the original problem, because  $\mathbf{C}$  cannot be factored into  $\mathbf{c}\mathbf{c}^T$ . It may still serve as a good

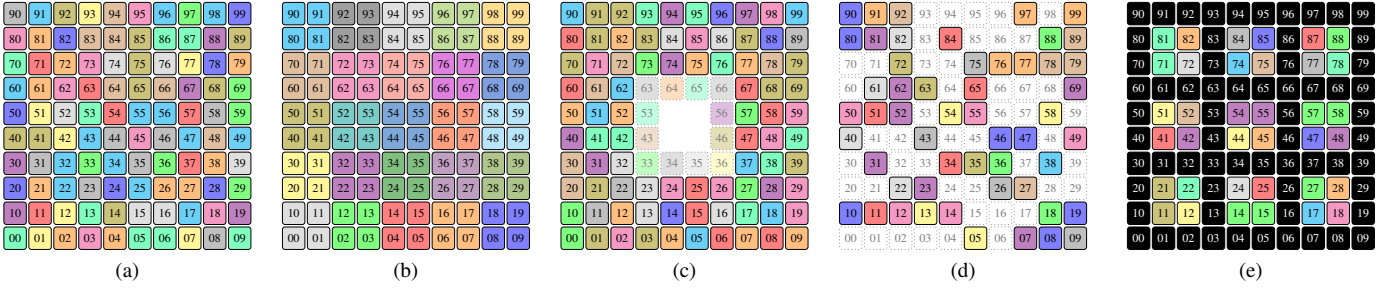


Fig. 3. Configurations of Sparse RIS (SRIS) considered in this paper: (a) fully tunable RIS, (b) parallel-connected  $2 \times 2$  clusters, (c)  $2 \times 2$  or  $4 \times 4$  center removed, (d) a random selection of 50% or 75% of the elements, and (e) nine  $2 \times 2$ -subregions with the other antennas short-circuited.

starting point for another algorithm to find a suitable "next-best" feasible solution. However, it cannot be proven that the solution found in this way is actually the optimal solution to the original problem.

#### IV. SIMULATION EXAMPLES

##### A. Setup

The simple  $10 \times 10$ -element printed dipole surface, shown in Fig. 2, serves as illustrative test case. The dipoles are modeled using finite-conductivity sheets (copper conductivity) to account for losses. They are uniformly separated by  $\lambda/2$  at the operating frequency of 3.75 GHz and lie on a 1.6 mm thick FR4 substrate backed by a layer of perfect conductor.

The transmit and receive antennas are two standard pyramidal horn antennas with about 16 dB gain. Their distance to the RIS is always  $d = 2D^2/\lambda$  (with  $D$  being the diagonal of the surface), such that far-field conditions apply. However, this is not a requirement for the method.

Note: While it is certainly computationally expensive to obtain the  $102 \times 102$  impedance matrix of the entire system, such simulations are often carried out at some point during the design of such a surface. Moreover, approximative methods could be used in the far-field.

##### B. SRIS Configurations

The following four SRIS configuration types, depicted in Fig. 3(b)–(e), are compared to the full RIS, shown in Fig. 3(a):

- parallel-connected  $2 \times 2$ -element clusters,
- removing a  $2 \times 2$ - or a  $4 \times 4$ -element center,
- randomly enabling 75% or 50% of all elements,
- nine  $2 \times 2$ -element subarrays, the other elements shorted.

The case with all RIS elements open-connected, i.e., predominantly a perfectly conducting square reflector with an RCS of about 17 dB in the normal direction, serves as base reference.

##### C. Results

1) *Tightness*: First of all, the graphs in Fig. 4 reveal that the relaxation was tight in all cases. Thus, indeed, the optimum solution of the QCQP (7) has been found at every point.

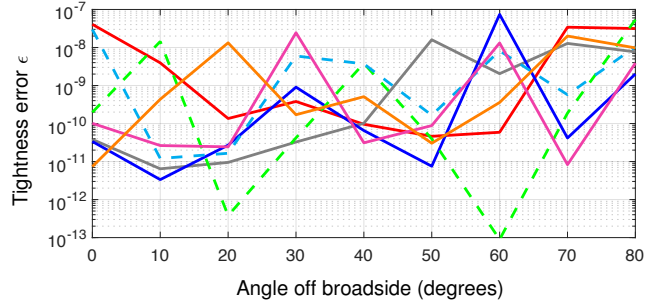


Fig. 4. These small tightness errors confirm that the relaxations are tight in all cases and that the optimum of the nonconvex QCQP (7) has been found at every point. See Fig. 5 for a legend.

2) *Optimized BRCS*: Using the equivalence between (2) and (3), the bistatic radar cross section is calculated from the obtained maximum PTE values. They are displayed vs. the angle off broadside to the RIS  $\alpha$  in Fig. 5, when the angle of incidence (transmit antenna) is constant  $\beta = -10^\circ$ .

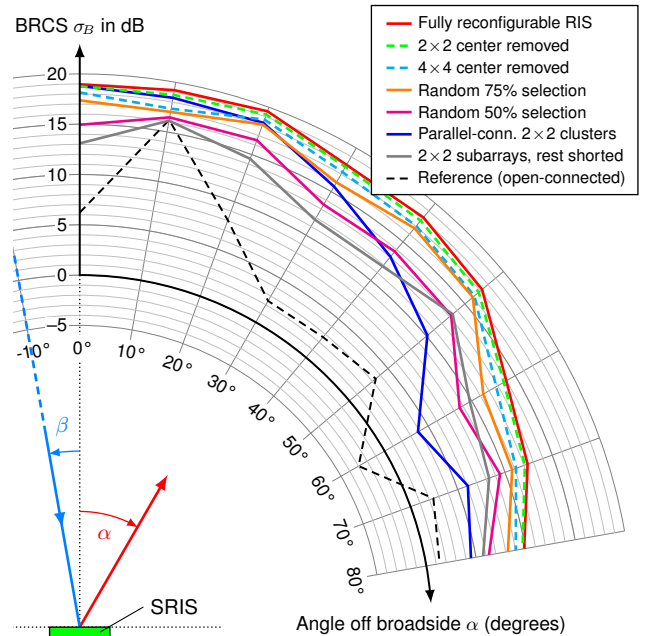


Fig. 5. The resulting bistatic radar cross section (BRCS) of the RIS, calculated from the maximum PTE values, for different SRIS configurations and angles  $\alpha = 0 \dots 80^\circ$  off broadside; constant angle of incidence  $\beta = -10^\circ$ .

As can be seen by the dashed green line, removing the four center elements has negligible effect, the larger center (dashed blue) reduces the BRCS by 1-2 dB. Saving these additional 10% of reconfigurable elements comes at a (small) price.

Reducing the SRIS randomly by 25% of its reconfigurable elements has a larger effect, but the SRIS can still provide a significantly larger BRCS, also at angles far off broadside. Even with only 50% reconfigurable elements, the SRIS still manages to provide a substantially improved BRCS compared to the reference reflector, which only provides the specular reflection at  $+10^\circ$ , as expected.

The SRIS that results from parallel-connected  $2 \times 2$  clusters, i.e., essentially an RIS of similar size but with only 25 instead of 100 reconfigurable elements, performs very well for small angles of reflections and only at angles beyond  $45^\circ$  starts falling behind. Lastly, 36 reconfigurable elements in nine  $2 \times 2$ -subarrays can provide better performance at flat angles, but falls behind at steep angles.

There is no clear winner at this point, but a few of these strategies definitely deserve further investigation.

## V. SUMMARY & CONCLUSION

First, this paper introduces the concept of Sparse Reconfigurable Intelligent Surfaces (SRIS): While RIS could play a crucial role in future wireless networks to enhance both coverage and energy efficiency, a large number of reconfigurable elements (e.g., varactor diodes as tunable capacitors) may prevent the second reason. Reducing the number of reconfigurable elements clearly affects the overall performance, while improving energy efficiency. This trade-off needs to be studied carefully, to find an optimal consensus.

Second, the versatile maximum power transfer optimization framework is adapted and applied to SRIS configurations to find their optimal performance and provide helpful insight for finding the aforementioned consensus between number and placement of reconfigurable elements and the performance of the SRIS. As shown, the involved relaxation is tight in all these cases, which means that the global maximum in terms of performance, measured via bistatic radar cross section (BRCS), and the corresponding optimal loading reactances could be found each time.

Finally, preliminary results show that different configurations to achieve the desired sparsity have different effects on reducing the number of reconfigurable components and the resulting RIS performance. This opens the way for further investigations, possibly also including constraints on maximum reflection levels in undesired directions.

## ACKNOWLEDGMENT

This work was carried out as part of the collaborative CHIST-ERA project "Towards Sustainable ICT: Sparse Ubiquitous Networks based on Reconfigurable Intelligent Surfaces (SUNRISE)". The authors of OST are supported by the Swiss National Science Foundation (SNF) with Grant 203784.

- [1] S. Hu, F. Rusek, and O. Edfors, "Beyond Massive MIMO: The potential of data transmission with large intelligent surfaces," *IEEE Trans. Signal Processing*, vol. 66, no. 10, pp. 2746–2758, 2018. doi: 10.1109/TSP.2018.2816577
- [2] C. Huang, A. Zappone, G. C. Alexandropoulos, M. Debbah, and C. Yuen, "Reconfigurable intelligent surfaces for energy efficiency in wireless communication," *IEEE Trans. Wireless Commun.*, vol. 18, no. 8, pp. 4157–4170, 2019. doi: 10.1109/TWC.2019.2922609
- [3] M. Di Renzo *et al.*, "Smart radio environments empowered by reconfigurable intelligent surfaces: How it works, state of research, and the road ahead," *IEEE J. Select. Areas Commun.*, vol. 38, no. 11, pp. 2450–2525, 2020. doi: 10.1109/JSAC.2020.3007211
- [4] Q. Wu and R. Zhang, "Towards smart and reconfigurable environment: Intelligent reflecting surface aided wireless network," *IEEE Commun. Mag.*, vol. 58, no. 1, pp. 106–112, 2020. doi: 10.1109/MCOM.001.1900107
- [5] C. Huang *et al.*, "Holographic MIMO surfaces for 6G wireless networks: Opportunities, challenges, and trends," *IEEE Wireless Communications*, vol. 27, no. 5, pp. 118–125, 2020. doi: 10.1109/MWC.001.1900534
- [6] W. Saad, M. Bennis, and M. Chen, "A vision of 6G wireless systems: Applications, trends, technologies, and open research problems," *IEEE Network*, vol. 34, no. 3, pp. 134–142, 2020. doi: 10.1109/MNET.001.1900287
- [7] Y. Liu *et al.*, "Robotic communications for 5G and beyond: Challenges and research opportunities," *IEEE Commun. Mag.*, vol. 59, no. 10, pp. 92–98, 2021. doi: 10.1109/MCOM.111.2001118
- [8] S. V. Hum and J. Perruisseau-Carrier, "Reconfigurable reflectarrays and array lenses for dynamic antenna beam control: A review," *IEEE Trans. Antennas Propagat.*, vol. 62, no. 1, pp. 183–198, 2014. doi: 10.1109/TAP.2013.2287296
- [9] H. Taghvaei, S. Terranova, N. M. Mohammed, and G. Gradoni, "Sustainable multi-user communication with reconfigurable intelligent surfaces in 5g wireless networks and beyond," in *16th European Conf. on Antennas and Propagation (EuCAP 2022)*, 2022, pp. 1–5. doi: 10.23919/EuCAP53622.2022.9769001
- [10] O. Tsilipakos *et al.*, "Toward intelligent metasurfaces: The progress from globally tunable metasurfaces to software-defined metasurfaces with an embedded network of controllers," *Advanced Optical Materials*, vol. 8, no. 17, p. 2000783, 2020. doi: https://doi.org/10.1002/adom.202000783
- [11] F. Yang and Y. Rahmat-Samii, Eds., *Surface Electromagnetics: With Applications in Antenna, Microwave, and Optical Engineering*. Cambridge University Press, 2019. ISBN 978-1-108-47026-1
- [12] H.-D. Lang and C. D. Sarris, "Optimization of wireless power transfer systems enhanced by passive elements and metasurfaces," *IEEE Trans. Antennas Propagat.*, vol. 65, no. 10, pp. 5462–5474, 2017. doi: 10.1109/TAP.2017.2735452
- [13] H.-D. Lang and C. D. Sarris, "Corrections to "Optimization of wireless power transfer systems enhanced by passive elements and metasurfaces,"" *IEEE Trans. Antennas Propagat.*, 2022. doi: 10.1109/TAP.2022.3199495
- [14] H.-D. Lang and C. D. Sarris, "From optimization of near-field WPT systems to far-field antenna arrays," in *2017 IEEE Internat. Symposium on Antennas and Propagation & USNC/URSI Nat. Radio Science Meeting*, 2017, pp. 141–142. doi: 10.1109/APUSNCURSINRSM.2017.8072113
- [15] M. A. Nyffenegger, C. D. Sarris, and H.-D. Lang, "Convex optimization of reactively loaded antenna arrays with backlobe and sidelobe constraints," in *16th European Conf. on Antennas and Propagation (EuCAP 2022)*, 2022, pp. 1–5. doi: 10.23919/EuCAP53622.2022.9769334
- [16] J. Xu, Y. Liu, X. Mu, and O. A. Dobre, "STAR-RISs: simultaneous transmitting and reflecting reconfigurable intelligent surfaces," *IEEE Commun. Lett.*, vol. 25, no. 9, pp. 3134–3138, 2021. doi: 10.1109/LCOMM.2021.3082214
- [17] Y. Liu *et al.*, "STAR: Simultaneous transmission and reflection for  $360^\circ$  coverage by intelligent surfaces," *IEEE Wireless Communications*, vol. 28, no. 6, pp. 102–109, 2021. doi: 10.1109/MWC.001.2100191
- [18] S. Boyd and L. Vandenberghe, *Convex Optimization*. Cambridge University Press, March 2004. ISBN 978-0-521-83378-3
- [19] R. H. Tütüncü, K. C. Toh, and M. J. Todd, "Solving semidefinite-quadratic-linear programs using SDPT3," *Mathematical Programming*, vol. 95, pp. 189–217, 2003. doi: 10.1007/s10107-002-0347-5